Vol. 19(2), pp. 127-136, April-June, 2024
DOI: 10.5897/IJPS2022.4978
Article Number: CD204D972297
ISSN: 1992-1950

http://www.academicjournals.org/IJPS

ACADEMIC JOURNALS
expand your knowledge

International Journal of Physical Sciences

Full Length Research Paper

The nexus between land surface temperature and vegetation condition: The case of Addis Ababa, Ethiopia

Dagnachew Sisay Chaka* and Binyam Tesfaw Hailu

[1]Department of Urban and Regional Planning, Faculty of Civil and Built Environment, Hawassa University, Hawassa, Ethiopia.
[2]Department of Remote Sensing and Geo-informatics, College of Natural and Computational sciences, Addis Ababa University, Addis Ababa, Ethiopia.

Received 26 January, 2022; Accepted 4 July, 2022

Examining the spatial relationship of surface temperature and Normalized Difference Vegetation Index (NDVI) in the urban center helps to balance heat island effect and creates sustainable urban environment. This study identifies the relationship between vegetation condition and surface temperature of Addis Ababa over various land use/cover (LU/LC) types. For this purpose, Landsat 8 OLI and TIR sensor data which were obtained in a dry season are used. The Land Surface Temperature (LST) of the area was retrieved by having surface emissivity that was derived from NDVI threshold method. The LST result of the city shows that the surface temperature of the city varied from 291.61 to 313.06 Kelvin (K). Within the city a significant change in surface temperature was observed over various LU/LC types, which is inversely proportional to their respective vegetation condition. The highest surface temperature and the lowest NDVI were registered on paved surfaces, bare land and settlement areas have lower NDVI value respectively. Whereas, forest and vegetative areas have low surface temperature and high NDVI as compared to the other land use and land cover types. Following the poor distribution of healthy vegetation in the city, the surface temperature varied from the center of the city where it has low NDVI in settlement areas to the peripheral zones. Therefore, to create a livable urban environment, we need sufficient land development regulation which should be friendly to the urban climate such as adding to the numbers of green places in parcels and city level that can attribute to the betterment of the climatic condition in the settlement area.

Key words: Addis Ababa, Ethiopia, Landsat 8, Land Surface Temperature (LST), Normalized Difference Vegetation Index (NDVI).

INTRODUCTION

The spatial variation of healthy vegetation (NDVI) has a major impact on natural resource management and environmental change monitoring (Ahmed, 2016; Worku et al., 2019). Various studies show that the NDVI and land surface temperature value have a strong negative correlation (Rehman et al., 2015; Chaithanya et al., 2017; Suresh and Mani, 2017). Areas with healthy vegetation and dense cover have the lowest mean LST and highest

*Corresponding author. E-mail: dagnuonline@gmail.com; Tel: +251910930163.

mean NDVI while non-vegetated areas like bare lands or paved surfaces have the highest LST and lowest mean NDVI (Sun et al., 2011) which implies that lower LST is usually measured in areas with higher NDVI values. The temperature is greater in areas that have lower healthy vegetation cover (Sruthi and Aslam, 2015). These indicate that land surface temperature (LST) is sensitive to vegetation cover (Chaithanya et al., 2017); the vegetation cover can reduce LST (Sruthi and Aslam, 2015). Besides, other studies prove that the variation of skin temperature over various LU/LC types depends on vegetation condition and is also determined by the elevation of the area and its geological setting (Chaka and Oda, 2021).

The development of different thermal sensors and number of thermal bands together with their LST modelling algorithms are supporting the visualization and determination of thermal characteristics of different surface structures. Following the number of thermal bands and atmospheric sensitivity of the sensors, the following algorithms such as, split window, single Chanel, mono-window, improved split window, improved mono window and radiative transfer equation-based method are commonly used (Yu et al., 2014). However, a proper algorithm for retrieving LST from different sensors thermal band still remains unavailable due to many difficulties in the atmospheric correction (Abutaleb et al., 2014; Wang et al., 2015). Currently, most researchers that use the Landsat 8 TIRS data are using improved mono-window algorithm. This algorithm is developed by modifying the existing mono-window algorithm following the calibration problem of Band 11 thermal data of Landsat 8 TIR caused by stray light (Sobrino and Raissouni, 2010; Sobrino et al., 2004; Abutaleb et al., 2014; Wang et al., 2015). There is also an easy method that the present study used, it was initially developed by Avdan and Jovanovska (2016) by considering the notice of USGS not to use band 11 of TIRS.

The thermal properties of building materials, urban geometric design, existing land-use/land-cover, altitudes and heat from anthropogenic (heat from factories, vehicles and air conditioners) are some of the factors that contribute to Urban Heat Island (UHI) phenomenon in urban areas. This mainly appears in the spatial distribution of LST which is governed by surface heat fluxes (Odindi et al., 2015; Oke, 1988; Rizwan et al., 2008; Dewan and Corner, 2012).

Conversely, it seems that the vegetation condition in settlement areas is contributing for the spatial variation of LST, and this issue is not seen in the other land use/land cover type. This variation will finally lead to examine Urban Heat Island effect resulted from high surface reflectance and vegetation conduction of an area (Dewan and Corner, 2012). Therefore, the spatial variation of land surface temperature and preparation of context-based mitigation strategies for cities, provide a multi directional decision-making skill for spatial planners which will help to ensure the quality of urban environment. However, in the proposed study area there is no any related recent studies. As a result of this, the effect of scientific results to raise awareness was not experienced. Results were not seen in decisions that change the warming local climate. Therefore, this study is expected to raise the local knowledge on how to balance the local economic development and their impact on heat island variation.

The goal of this study is to explore the relationship of the vegetation condition (NDVI) and LST, using thermal remote sensing data that represent the real spatial pattern of land surface temperature on heterogeneous urban environment. Specifically, this paper has the following 3 objectives: these are (1) to estimate land surface temperature of the study area; (2) to examine the relationship between land surface temperature and NDVI and (3) to examine the impact of urban development of an area on the spatial variation Urban Heat Island.

METHODOLOGY

Description of the study area

Considering the rapid urbanization, industrial development and richness to various LU/LC distribution pattern, Addis Ababa has been selected as the study area for this research. As shown in Figure 1, the city is located between latitude of 9.02497°N and longitude of 38.74689°E and has a subtropical highland climate. The city has a complex mix of highland climate zones, with temperature differences of up to 10°C (18°F), and with average elevation of about 2,355 m above the mean sea level. It is a capital of Ethiopia and a seat for various administrative organizations. It has an area of 54,000 ha. Addis Ababa is bounded by ‘Ehntoto’ mountain that has high density of eucalyptus tree in the norther direction and high industrial development in the south with flat topography. The city is growing very fast and transformed from a very small population to a city of multi-million population and a major industrial center due to this phenomenon the climatic condition of the city is changing dramatically. Figure 1 illustrates the location of the study area.

Data sources

Table 1 describes three different data’s that were used for this study. However, the major remote sensing data is Landsat 8 thermal infrared (band 10), that has high atmospheric transitivity value. The month of November is selected for the acquisition of these images, as it is harvesting season for the acquisition of less cloud cover and high-quality satellite data of the area with a spatial resolution 100 m is selected for LST retrieval, and the data has no calibration problem caused by stray light. To find out the relation that exist between LST and each land cover in the study area, multispectral image of the same time were used. The overall analysis of the project is done using ERDAS IMAGINE 2015, ENVI version 5.1 and ArcGIS 10.5 software.

Methods

In order to achieve the objective of the study both qualitative and quantitative techniques were applied on the analysis results of thermal data. Both Landsat 8 OLI and TIRS had atmospheric errors. Hence, pre-processing was undertaken before any further analysis and extraction of information from satellite images. For the

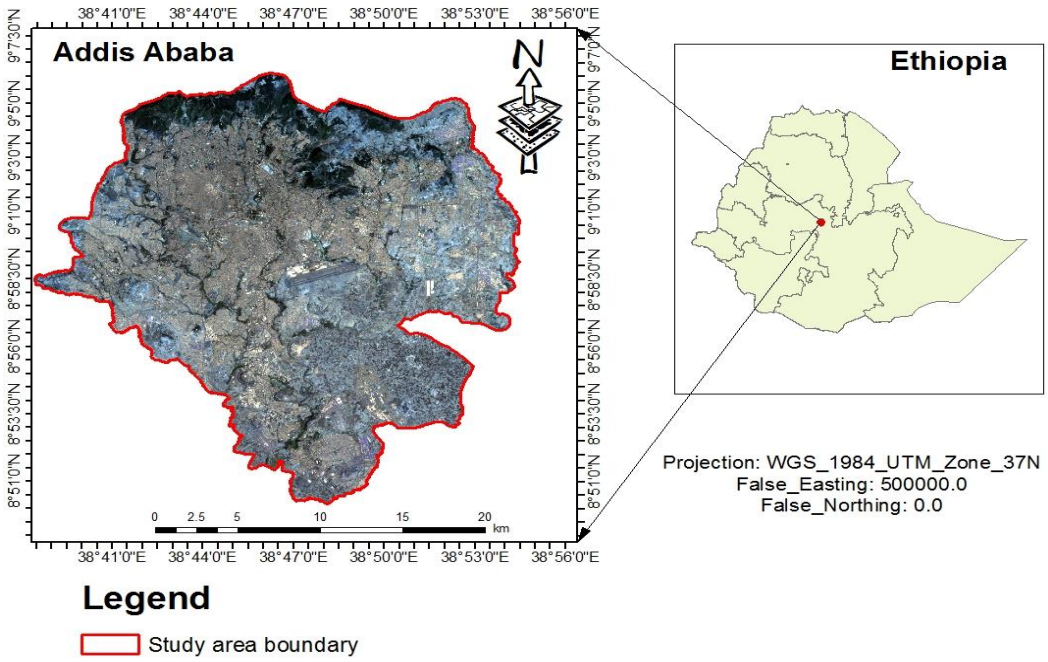

Figure 1. Location map of study area.
Source: Map done by researchers

Table 1. Overview of the data set used for the study.

Data set	Acquisition date	Source	Data type	Purpose of the data
Landsat 8 OLI /TIRS with a path/row 168/054	2017/10/02	USGS	Landsat 8 OLI	Determination of NDVI, emissivity
	2017/10/02	USGS	Landsat 8 TIRS	Estimation of LST
Sample data	2017	Google earth	Point data	For supervised classification and validation

Source: prepared by researchers

pre-processing of Landsat 8 OLI image, ENVI 5.1 was used. Before the extraction of information, the Landsat 8 OLI and TIRS were resampled to 30 m × 30 m using the nearest neighborhood resampling method. For the classification and derivation of LST from land surface emissivity and vegetation proportion values ERDAS IMAGINE 2015, ENVI 5.1 and Arc GIS 10.5 software package were used.

Image classification

For the purpose of this paper, the land use/cover of the area were classified into five different classes considering the distribution of green cover using the pre-processed of Landsat 8 OLI image of the area. These LU/LC types were prepared using supervised classification under maximum likelihood algorithm. These are vegetation, settlement, road and paved surface, bare land (including barren and vacant land), and agriculture and grass land.

Estimation of land surface temperature

The present study used an easy method developed by Avdan and Jovanovska (2016); this is used by considering the notice of USGS not to use band 11 of TIRS. This method has four (4) main stages for the estimation of land surface temperature of the area. These are:

Conversion of at sensor thermal spectral radiance (L_λ): The formula used in the process to convert the digital numbers into radiance was the next equation (Wang et al., 2015).

$$L_\lambda = M_{10}\, Q_{10} + A_{10} - O_{10} \quad (1)$$

where Lλ is the spectral radiance of the thermal band 10 in $W{\cdot}m^{-2}{\cdot}sr^{-1}{\cdot}\mu m^{-1}$, M_{10} is the band-specific multiplicative rescaling factor for band 10, A_{10} is the band-specific additive rescaling factor for band 10, Q_{10} is the DN value for the quantized and calibrated standard product pixel of band 10, whereas O_{10} is the correction for band 10 issued by USGS for the calibration of TIRS bands of Landsat 8 TIRS before February 3, 2014, is 0.29 ($W{\cdot}m^{-2}{\cdot}sr^{-1}{\cdot}\mu m^{-1}$). However, the data used for the estimation of LST was acquired after this date; as a result this value has not been considered (Wang et al., 2015). Table 2 show the value for the coefficient M10 and A10 that were obtained from the Metadata file of the image.

Table 2. Determination of constants from the metadata file of the Landsat 8 TIRS Band 10.

Landsat8 PRODUCT_ID	M_{10}	A_{10}	K1 ($W \cdot m^{-2} \cdot sr^{-1} \cdot \mu m^{-1}$)	K2 ($W \cdot m^{-2} \cdot sr^{-1} \cdot \mu m^{-1}$)
"LC08_L1TP_168054_20171002_20171002_01_T1"	3.3420E-04	0.10000	774.8853	1321.0789

Source: prepared by researchers

Determination of surface brightness temperature (BT): The thermal spectral radiance (L_λ) value were converted to BT using the constants obtained from the metadata file using the next equation (Tan et al., 2010b).

$$BT = \frac{K2}{\ln\left(1+\frac{K1}{L\lambda}\right)} - 273.15$$

where BT is brightness temperature (°C); L_λ is thermal spectral radiance for Landsat 8 TIRS band 10 data; K1 and K2 are constants obtained from the metadata file in $W \cdot m^{-2} \cdot sr^{-1} \cdot \mu m^{-1}$ (Table 2).

Determination of ground Emissivity (ε_λ) using NDVI: Surface emissivity of the area was calculated based on the NDVI threshold. Three different stages were passed through to determine the ground emissivity of the surface as follows.

(A) Determination of the vegetation condition of the area from the multispectral satellite data of Landsat 8 OLI using the visible (red) band data (band 4) and near infrared (NIR) band (band 5) portion of the spectrum using the equation (Burgan and Hartford, 1993).

$$NDVI = \frac{NIR\ (band\ 5) - RED(band\ 4)}{NIR\ (band\ 5) + RED(band\ 4)} \quad (3)$$

(B) Derivation of vegetation proportion (Pv) of the area using the next equation (Quintano et al., 2015).

$$Pv = \left(\frac{NDVI - NDVIs}{NDVIv - NDVIs}\right)^2 \quad (4)$$

where P_v is the proportion of vegetation; NDVIv and NDVIs is the suggested NDVI values for vegetation and soil (NDVIv = 0.5 and NDVIs =0.2) that were applied to determine the value of P_v, respectively (Avdan and Jovanovska, 2016; Sobrino et al., 2004). Whereas, NDVI is the vegetation condition of the area obtained from Equation 3.

(C) Determination of ground emissivity of the band using the next equation (Sobrino et al., 2004)

$$\varepsilon_\lambda = \varepsilon_{v\lambda} Pv + \varepsilon_{s\lambda}(1 - Pv) + C_\lambda \quad (5)$$

$$\varepsilon_\lambda = \begin{cases} \varepsilon_{s\lambda}, & NDVI < NDVIs \\ \varepsilon_{v\lambda} Pv + \varepsilon_{s\lambda}(1 - Pv) + C_\lambda, & NDVIs \leq NDVI \leq NDVIv \\ \varepsilon_{s\lambda} + C_\lambda, & NDVI \geq NDVIv \end{cases} \quad (6)$$

where $\varepsilon_{v\lambda}$ and $\varepsilon_{s\lambda}$ are emissivity of vegetation and soil, respectively, and the surface roughness is represented by a constant C_λ, which is taken as a constant value of 0.005. However, for homogenous and flat surfaces the value of C_λ = 0 (Jeevalakshmi et al., 2017; Sobrino and Raissouni, 2010), whereas Pv is the vegetation proportion obtained from Equation 4. Finally, the condition can be represented with Equation 6 and the ground emissivity of the band was determined as a mean of four land-use/land-cover types of the area (Table 3).

Mapping of surface temperature (Ts): Finally, Land Surface Temperature (LST) of the area was estimated using the following formula:

$$Ts = \frac{BT}{\left\{1 + \left[\left(\frac{\lambda BT}{\rho}\right) \ln \varepsilon\lambda\right]\right\}} \quad (7)$$

where Ts is the land surface temperature in (°C), BT is at-sensor brightness temperature in (°C), λ is the wavelength of emitted radiance (for which the peak response and the average of the limiting wavelength (λ=10.895) were used) (Markham and Barker, 1985), and ε_λ is the ground emissivity and ρ was calculated using the next formula:

$$\rho = h\frac{c}{\sigma} \quad (8)$$

where σ is the Boltzmann constant (1.38×10^{-23} J/K); h is Planck's constant (6.626×10^{-34} J s), and c is the velocity of light (2.998 × 108 m/s) (Avdan and Jovanovska, 2016; Weng et al., 2004).

RESULTS

Land use land cover map of Addis Ababa

The LU/LC map of the area is prepared with an overall accuracy of 81.73% and a Kappa of 0.812. As shown in Figure 2, the large coverage of green vegetation or urban forest is found around the northern parts of the city, which is locally known as "Ehntoto "and" Yeca Mountain. Whereas, the other parts of the city have fragmented vegetation, these are along the river side, within the embassies and churches compound. Whereas, the other parts of the city are dominated by high density of built-up areas. As of Rahman et al. (2006), the classification result in the period is done with strong agreement and taken as reliable data for this study, because, the classification has a Kappa coefficient greater than 0.8.

Table 4 shows the total area coverage of land use land cover type, among these the settlement area covers the largest area of the city with an area of 27737 ha, whereas paved surface that contributes a lot for urban heat island variation covers the second highest value (7493 ha) from the total area of the city. However, the distribution of green vegetation such as forest, grass and agricultural land that lower the warming local climate are poorly distributed and have lower area coverage.

Table 3. Overview for the determination of ground emissivity of Landsat 8 band 10 data using the NDVI value.

Land-use/land-cover	NDVI	Ground emissivity
Water	< 0	0.971
Bare soil (fallow land)	0-0.2	0.986
Grass, shrubs and sparsely distributed urban vegetation	0.2-0.5	Determined using the above formula (Equation 5)
Woody vegetation	> 0.5	0.991

Source: Jeevalakshmi, D., S. Narayana Reddy and B. Manikiam (2017). Land Surface Temperature Retrieval from Landsat data using Emissivity Estimation.

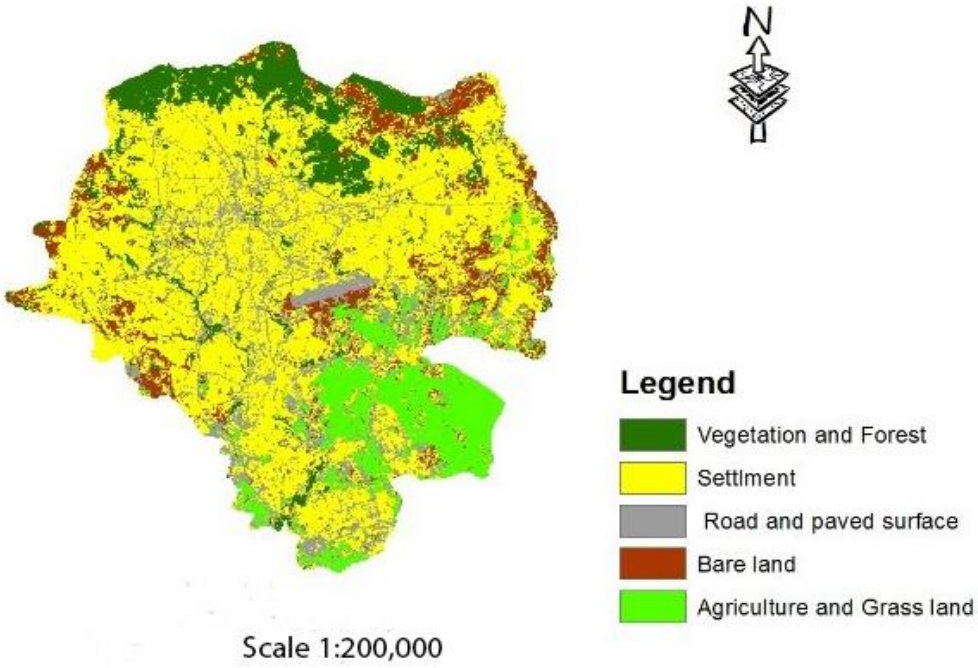

Figure 2. Land use/Land cover map of Addis Ababa.
Source: Map done by researchers

Table 4 LU/LC area coverage.

Land use/Land cover	Area (ha)
Vegetation and forest	5937.57
Settlement	27737.46
Road	7493.49
Bare or vacant land	4940.1
Agriculture and grass land	5831.37

Source: prepared by researchers

Spatial pattern of NDVI and emissivity of Addis Ababa

Figures 3 and 4 show the vegetation condition and surface emissivity of Addis Ababa. As shown in Figure 3, the northern parts of the city (around 'Ehntoto' mountain) has high NDVI value. This area is characterized by high vegetation distribution and low surface reflectance. Whereas, areas to the south and south east are characterized by a very low vegetation distribution and high surface reflectance. As a result, the NDVI value of these areas is relatively lower as compared to the other parts of the city. Since the image used was acquired in a dry season, those areas with lower vegetation and high surface reflectance have a NDVI value less than 0.2, whereas areas to the northern parts of the city, embassies and river sides have higher NDVI value that measures more than 0.5 and surface emissivity above 0.7 (Figure 4).

The spatial pattern of emissivity in Figure 4 shows similar pattern of distribution with NDVI in the study area. This map shows areas that have the value closer to 1 as high emissivity. This figure shows the effectiveness of the surface in emitting energy as radiation. Therefore, areas that have high NDVI show high emittance whereas emissivity close to 0.5 shows low emittance and a very

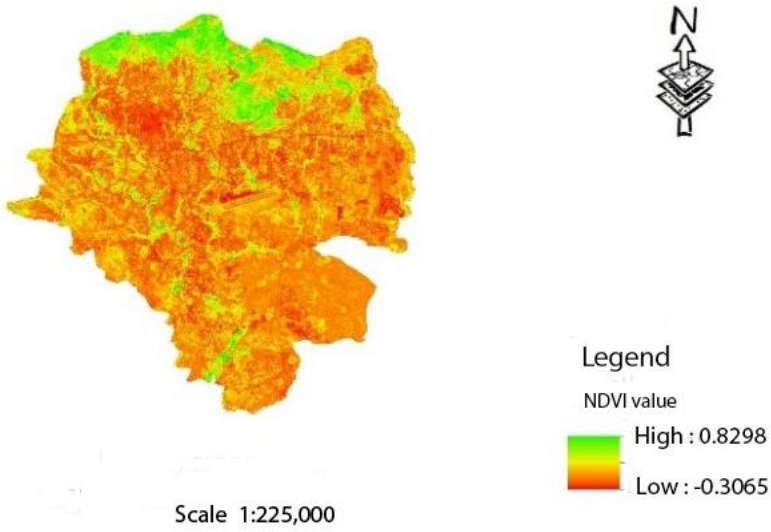

Figure 3. Spatial pattern of vegetation condition (NDVI).
Source: Map done by researchers

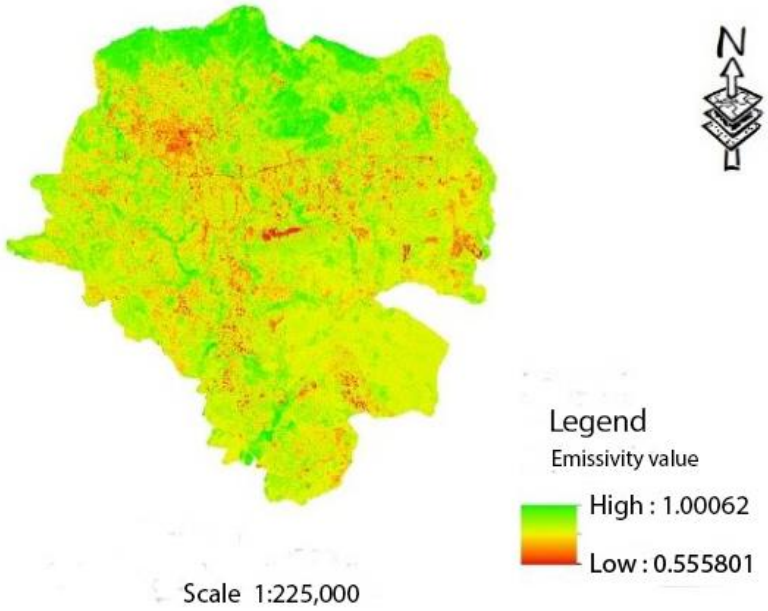

Figure 4. Distribution of surface emissivity.
Source: Map done by researchers

low NDVI value (Figures 3 and 4).

Spatial pattern of LST of Addis Ababa

The map of LST shows the intensity of the spatial pattern of surface temperature in a 2D map. The comparison results with MODIS day time proves that the estimated result from Landsat 8 TIRS band 10 is consistent because the variation is below 2k (Yosef et al., 2017). As shown in the map the LST of the city gradually changes from north end to south, following the change in land use land cover type and the spatial variation of NDVI. The maximum LST of the area is measured 291.61 and the minimum land surface temperature of the city is 313.06 Kelvin (K). The minimum temperature was recorded in

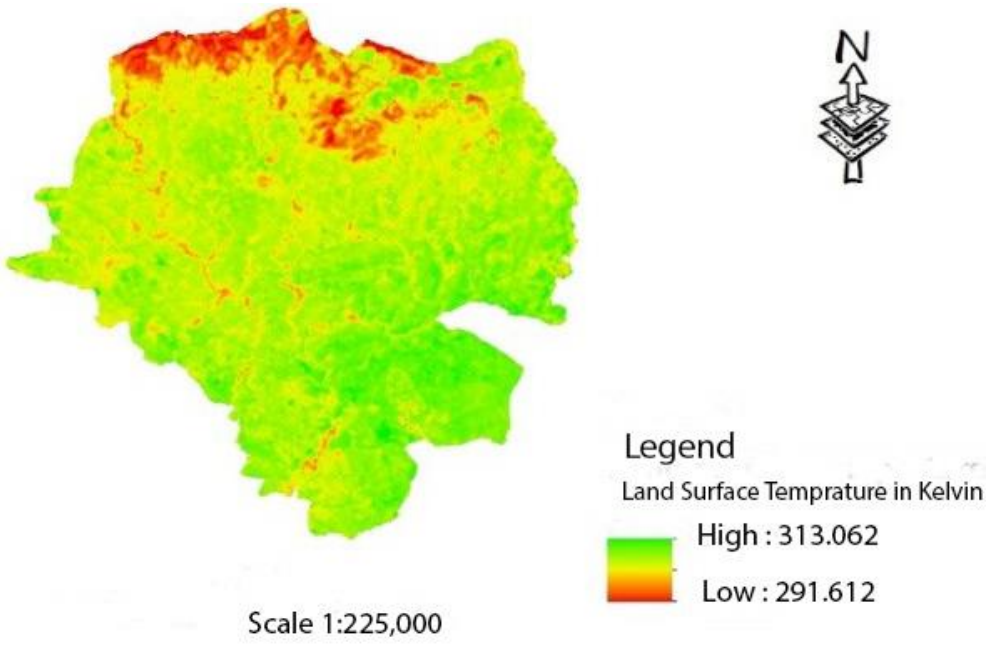

Figure 5. LST distribution pattern in Addis Ababa.
Source: Map done by researchers

Table 5. Distribution of mean LST, NDVI and emissivity over various land use land cover type.

Land use/Land cover type	NDVI	Emissivity	LST (K)
Vegetation and forest	0.5978	0.9852	296.577
Settlement	0.1045	0.9032	306.181
Agriculture and grass land	0.2398	0.9423	304.343
Paved surfaces	0.0575	0.8752	308.561
Bare or vacant land	0.1569	0.9223	306.744

Source: prepared by researchers

vegetated areas (around the northern parts) of the city (Figure 5).

Due to poor vegetation condition and high surface reflectance registered on vacant land, the maximum temperature was registered at the center of the city and peripheral areas. In addition, it is also registered at some parts of paved surfaces including Bole International airport of the city.

Comparison of LST, emissivity and NDVI over various LU/LC type

From the quantitative analysis result presented in Table 5, the highest surface temperature and the lowest NDVI and emissivity were observed on paved surfaces. Conversely, vegetation and forest areas had the lowest surface temperature and the highest NDVI and emissivity. Whereas, the other land use land cover types such as, bare land and settlement areas had high LST and low NDVI respectively. However, urban agricultural and grass lands of the city have low LST and High NDVI value as compared to the settlement and paved surfaces.

Correlation between LST and NDVI values

As depicted in the processed Landsat 8 TIRS, the northern parts of the city experiences low surface temperature. However, the southern and central parts of the city have relatively high LST, due to the shortage of healthy vegetation cover in the area. Whereas, areas to the east end have cold LST pattern as a result of high healthy vegetation cover. Therefore, a particular relationship that exists between LST and NDVI has been identified. As shown in Figure 6, NDVI and LST have

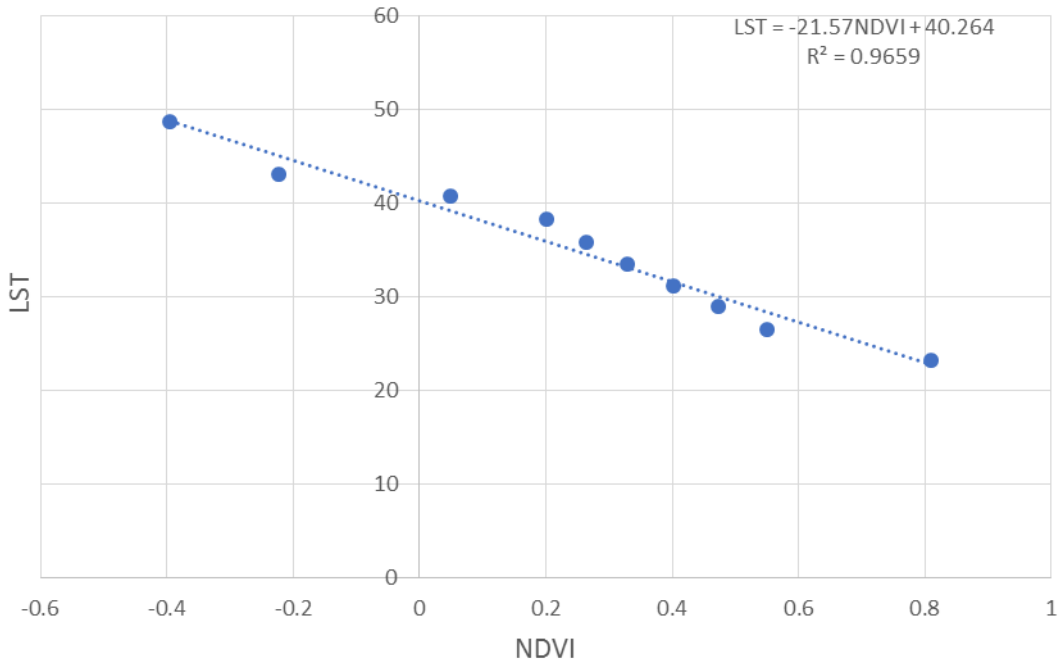

Figure 6. Correlation of LST with NDVI of Hawassa and its surroundings.
Source: Map done by researchers

strong negative linear correlation with the value of correlation measure (R2) 0.9659.

DISCUSSION

Impact factor of urban planning land use distribution pattern

The result shows that the type of impervious surfaces or built-up structures can have a different impact on emissivity. Among the five-land use type, the 'ehntoto' park and forest to the north of the study area has higher emissivity. The reason is that the theme forested and vegetated areas have higher vegetation cover and lower surface reflectance. For instance, the emissivity and NDVI of paved surfaces is 0.87 and 0.05, respectively. The density or NDVI of this area is below 50% of the other land uses, as its main function is for transportation. However, the emissivity and NDVI of settlement areas vary from place to place, and have the value of 0.9 and 01, respectively. This may be because of the existence of healthy vegetation distribution within the embassies, churches and the riverside green spaces. Vegetated areas to the northern part of the city have the highest values for both factors (Table 5). This is also because of the dense vegetation coverage in the area (Figure 2). Therefore, the distribution of healthy vegetation or NDVI is lower and lower as we go from the northern part of the city to the center and the southern end.

For the result of LST and its spatial pattern, we have similar conclusion. In each land use/land cover types, there is a change in surface temperature that ranges from 2 to 7K. This is due to a significant variation of NDVI observed within the land use/land cover type. However, the result observed on bare land may not only be associated with the existence of vegetation condition; it might be the nature of the surface. The research conducted by Belete (2017) at Adama Zuriya Woreda proves that, the LST result observed on bare land is the effect of the reflectance of the surface. Furthermore, the study identified that those surfaces that has low NDVI values during the dry season exhibited high surface reflectance. Similarly, these surfaces have high land surface temperature (Table 5).

Impact of healthy vegetation (NDVI) distribution pattern

The NDVI and LST regression coefficient of determination (R^2) is 0.96. This means these two phenomena have strong correlation. The spatial intensity of LST can be determined by the density and pattern of LST. As understood from Figures 3 and 5, areas that have high NDVI values have low LST and areas with low NDVI values have high LST. Different studies conducted on heterogeneous landscape areas prove that these two phenomena have negative correlation (Chaka and Oda, 2021; Worku et al., 2019). Besides, the negative effect

green coverage can have greeter cooling effect on heat island phenomenon (Sandor et al., 2019).

Conclusion

Following the mapping and quantitative results of LU/LC classes, NDVI and LST of Addis Ababa, several conclusions were made for varying related issues such as vegetation condition, relationship of land use land cover type and spatial variation of surface temperature. The NDVI value shows that the northern part of the study area and some parts of river side in Addis Ababa have relatively dense and healthy vegetation. Those areas that have high NDVI value also have high emissivity, which implies that it is directly proportional with healthy vegetation distribution. However, as we go down to the center of the city the distribution of healthy vegetation becomes fewer and fewer, this enforces the area to have high surface temperature.

The correlation measure of the two urban phenomena (NDVI and LST) suggests that they are predictive factors in the heat island pattern. The higher mean LST values of LU/LC type of the urban environment and lower mean values of healthy vegetated surfaces further confirm the association. As a result, the variations of land surface temperature are also indicators of the spatial patterns of urban heat island effects and vegetation cover. In general, the finding of this reserch shows that the spatial variation of LST in the study area is highly associated with LU/LC variation, the healthiness of vegetation (NDVI) distribution pattern, and other human induced activities. The LST values of the area were found to be as a good indicator of the spatial variation and status of NDVI of the particular area.

CONFLICT OF INTERESTS

The authors have not declared any conflict of interests.

REFERENCES

Abutaleb K, Adeline Ngie F, Ahmed MH, Ahmed SB, Elkafrawys SM, Arafat AD (2014). Investigation of urban heat island using Landsat data. In: Proceedings of the 10th Int. Cong, pp9, AARSE, University of Johannesburg, Wits University South Africa and National Authority for Remote Sensing and Space Sciences, Egypt.

Ahmed N (2016). Application of NDVI in vegetation monitoring using GIS and remote sensing in northern Ethiopian highlands. Abyss. Journal of Science and Technology 1(1):12-17.

Avdan U, Jovanovska G (2016). Algorithm for Automated Mapping of Land Surface Temperature Using Landsat 8 Satellite Data. Journal of Sensors. 2016:1-8. Article ID 1480307. http://dx.doi.org/10.1155/2016/1480307.

Belete T (2017). Impact of land-use/land-cover changes on land surface temperature in Adama Zuria Woreda, Ethiopia, using geospatial tools. Unpublished MSc thesis, Addis Ababa University, Addis Ababa, Ethiopia 91 p.

Burgan RE, Hartford RA (1993). Monitoring vegetation greenness with satellite data. Gen. Tech. Rep. INT-297. Ogden, UT: U.S. Department of Agriculture, Forest Service, Intermountain Research Station 13 p.

Chaithanya V, Binoy B, Vinod T (2017). Estimation of the relationship between urban vegetation and land surface temperature of Calicut city and suburbs, Kerala India using GIS and remote sensing data. International Journal of Advanced Remote Sensing and GIS 6(1):2088-2096.

Chaka DS, Oda TK (2021). Understanding land surface temperature on rift areas to examine the spatial variation of urban heat island: the case of Hawassa, southern Ethiopia. GeoJournal 86:993-1014. https://doi.org/10.1007/s10708-019-10110-5

Dewan A, Corner R (2012). The impact of land use and land cover changes on land surface temperature in a rapidly urbanizing megacity. In: Proceedings of the IEEE International Geoscience and Remote Sensing Symposium P 100. IGARSS, Munich, Germany.

Jeevalakshmi DS, Narayana R, Manikiam B (2017). Land Surface Temperature Retrieval from Landsat data using Emissivity Estimation. International Journal of Applied Engineering Research. 12(20):9679-9687.

Markham BL, Barker JL (1985). Spectral characterization of the Landsat thematic Mapper sensors, International Journal of Remote Sensing. 6(5):697-716.

Odindi JO, Bangamwabo V, Mutanga O (2015). Assessing the value of urban green spaces in Mitigating Multi-Seasonal urban heat using MODIS land surface temperature (LST) and Landsat 8 data. International Journal of Environmental Research 9:9-18.

Oke TR (1988). The urban energy balances. Progress in Physical Geography 12:471-508.

Quintano C, Fernández-Manso A, Calvo L, Marcos E, Valbuena L (2015). Land surface temperature as potential indicator of burn severity in forest Mediterranean ecosystems. International Journal of Applied Earth Observation and Geoinformation 36:1-12.

Rahman MM, Csaolovics E, Koch B, Kohl M (2006). Interpretation of Tropical Vegetation Using Landsat ETM+ Imagery, South-eastern Bangladesh.

Rehman Z, Kazmi SJH, Khanum F, Samoon ZA (2015). Analysis of land surface temperature and NDVI using geo-spatial technique: A case study of Keti Bunder, Sindh, Pakistan. Journal of Basic and Applied Sciences, 11:514-527.

Rizwan AM., Dennis YC, Liu C (2008). A review on the generation, determination and mitigation of urban heat island. Journal of Environmental Science, 20:120-128.

Sandor J, Istvan V, Huawei L, Guifang W, Krisztina Filep K (2019). Visualized relation of land use, ecological network and heat island: GIS based analysis and visualization in Hungarian pilot areas, pp 346

Sobrino JA, Raissouni N (2010). Toward Remote Sensing Methods for Land Cover Dynamic Monitoring: Application to Morocco, International Journal of Remote Sensing. 21(2):353-366.

Sobrino JA, Jiménez-Muñoz K, Leonardo JCP (2004). Land surface temperature retrieval from LANDAT TM5. Remote Sensing of Environment. 90(4):434-440.

Sruthi S, Aslam MM (2015). Agricultural drought analysis using the NDVI and land surface temperature data; a case study of raichur district. Aquat. Procedia 4:1258-1264.

Sun Q, Wu Z, Tan J (2011). The relationship between land surface temperature and land use/land cover in Guangzhou, China. Environmental Earth Science 65:1687-1694.

Suresh S, Mani K (2017). Application of remote sensing in understanding the relationship between NDVI and LST. International Journal of Renewable Energy Technology. 6(2):99-105.

Tan KC, San Lim H, MatJafri MZ, Abdullah K (2010). Landsat data to evaluate urban expansion and determine land use/land cover changes in Penang Island, Malaysia. Environmental Earth Sciences 60(7):1509-1521.

Wang F, Zhihao Qin, Caiying Song, Lili Tu, Arnon Karnieli and Shuhe Zhao (2015). An Improved Mono-Window Algorithm for Land Surface Temperature Retrieval from Landsat 8 Thermal Infrared Sensor Data, Remote Sens 7:4268-4289.

Weng QHD, Lu S, Schubring J (2004). Estimation of land surface temperature-vegetation abundance relationship for urban heat island studies, Remote Sensing of Environment. 89(4):467-483.

Worku N, Binyam TH, Aramde F (2019). An assessment of the vegetation cover change impact on rainfall and land surface temperature using remote sensing in a subtropical climate, Ethiopia.

Remote Sensing Application: Society and Environment 16(2019):100266.
Yosef M, Binyam T, Ameha A, Tesfaye K (2017). Detection of geothermal anomalies using Landsat 8 TIRS data in Tulu Moye geothermal prospect, Main Ethiopian Rift, The 4th National GIS Summit, 13-15 January 2017, The Geospatial Data and Technology Centre (GDTC) of Bahir Dar University Bahirdar, Ethiopia.
Yu X, Xulin G, Zhaocong Wu (2014). Land Surface Temperature Retrieval from Landsat 8 TIRS—Comparison between Radiative Transfer Equation-Based Method, Split Window Algorithm and Single Channel Method. Remote Sens 6:9829-9852.